W.-C. Li, Z. Ren, and C. T.-C. Nguyen, "A micromechanical high-*Q* elliptic disk displacement amplifier," *Tech. Digest*, 2016 IEEE Int. Micro Electro Mechanical Systems Conference, Shanghai, China, Jan. 24-28, 2016, pp. 663-666

A MICROMECHANICAL HIGH-*Q* ELLIPTIC DISK DISPLACEMENT AMPLIFIER

Wei-Chang Li[1], *Zeying Ren*[1,2], *and Clark T.-C. Nguyen*[1]
[1]Department of EECS, University of California, Berkeley, California, USA
[2]Now with Crossbar Inc., Santa Clara, California, USA

ABSTRACT

An 89-MHz micromechanical elliptic-disk displacement amplifying resonant switch ("resoswtich") (*cf.* Fig. 1(c)) with a displacement gain of 2.04 has achieved a *Q* of 101,600—more than 9× higher than that of previous array-based (Fig. 1(a) [1]) and slotted-disk (Fig. 1(b) [2] [3]) approaches. Key to this demonstration are: 1) gain-inducing axial stiffness differences derived from ellipse geometry rather than previous *Q*-degrading slots; and 2) an elliptic resonance strain field that better negates energy loss at a center anchor, allowing for *Q*'s even higher than circular disks. This ability to affect displacement amplification while maintaining *Q* >100,000 should provide more than 10-dB sensitivity improvement for recent resoswitch-based zero-quiescent radio receivers [4].

INTRODUCTION

The recent demonstration of a wireless receiver employing a micromechanical resoswitch (*cf.* Fig. 1) to permit continuous listening while consuming no power until a valid input signal arrives [4] has sparked renewed interest in ultra-low power sensor networks that dispense with the complexity of sleep/wake cycles and remain awake and listening at all times. Indeed, such a zero-quiescent power receiver, with block diagram pictured in Fig. 2, obviates the need for real-time clocks to synchronize the wake-up times of networked sensor motes, thereby eliminating their cost and power consumption.

Although the -60dBm sensitivity demonstrated in [4] is already sufficient for many short range wireless sensor applications, its 20-kHz frequency relegates it to low bit rate long-range applications, e.g., time transfer from an atomic reference (perhaps at NIST) to a portable clock thousands of miles away that receives atomic time via radio transmission in the 60-kHz LF WWVB band [5] [6]. To address more abundant higher bit rate applications, operation at higher frequencies spanning 60 MHz to 5.8 GHz is desirable.

Since (as shown in [4]) the sensitivity of a receiver like that of Fig. 2 is proportional to frequency and inversely proportional to the *Q* of its resoswitch, the *Q* of 10,500 achieved in [1] must rise to at least 100,000 if reasonable sensitivity is to be maintained at frequencies in the 80-100 MHz range. In addition, displacement amplification is desirable to not only prevent input impacting while promoting output impacting [7], but also to improve impedance matching and in some cases further improve sensitivity. Unfortunately, previously demonstrated displacement amplifying resoswitches in this frequency range suffer *Q* degradation, negating any sensitivity advantages. In particular, energy-balancing array-based resoswitches post *Q*'s of only 10,500 [1], while slotted-disk ones on the order of only 5,000 [2], the latter far lower than the >100,000 normally exhibited by their base resonator designs. In effect,

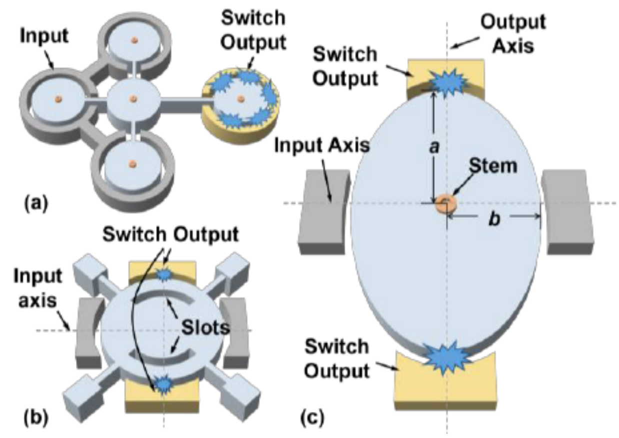

Type	Disp. Gain	Freq.	*Q*
(a) Array	2	153 MHz	~10,500
(b) Slotted-Disk	1.86	57 MHz	~5,000
(c) Elliptic-Disk	2.04	89 MHz	~101,600

Fig. 1: Descriptions of (a) array; (b) slotted-disk; and (c) elliptic-disk displacement amplifiers, along with a table comparing their performance, where the elliptic-disk displacement amplifier clearly presents the highest Q.

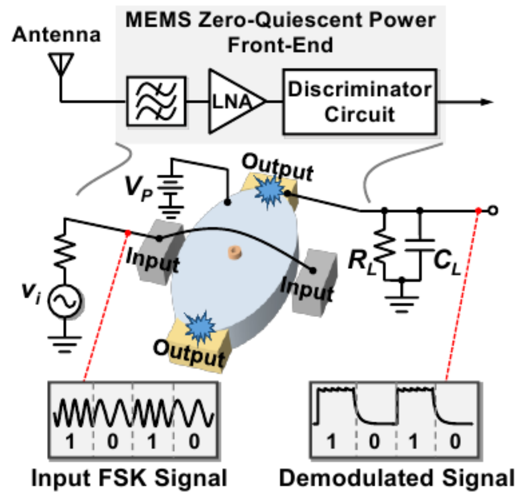

Fig. 2: Schematic of a resoswitch-enabled zero-quiescent power receiver architecture.

these devices sacrifice *Q* to attain displacement gain.

Pursuant to breaking the apparent *Q* versus displacement gain trade-off, this work presents an 89-MHz micromechanical elliptic-disk displacement amplifying resoswitch that preserves *Q* by 1) generating gain-inducing axial stiffness differences from ellipse geometry rather than previous *Q*-degrading slots; and 2) using an elliptic resonance strain field that better negates energy loss at a center anchor, allowing for *Q*'s in some cases even higher than circular disks. These strategies together permit a displacement gain of 2.04 with a *Q* of 101,600 more than 9× higher than that of previous array-based [1] and slotted-disk [2]

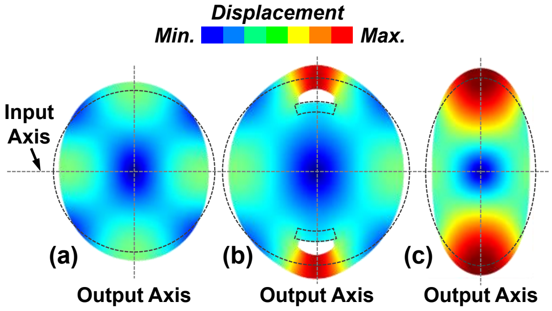

Fig. 3: FEM simulated mode shapes comparing displacements along input and output axes for (a) a conventional wine-glass disk resonator; (b) a slotted-disk displacement amplifier; and (c) an elliptic disk.

[3] approaches. Measurements reveal that the Q's of elliptic disks vary with ellipse aspect ratio (AR) defined as the major axis length a to the minor axis b, shown in Fig. 1(c). Specifically, a 95-MHz ellipse with AR = 1.2 (a/b = 21.91 μm/18.26 μm) exhibits the lowest Q, while one with AR = 1.6 and beyond restores the Q to equal or sometimes exceed that of a circular disk with AR = 1.

ADVANTAGES OVER PREVIOUS RESOSWITCHES

Fig. 1 compares the present elliptic design in (c) with previously-demonstrated displacement amplifying methods based on (a) energy-balanced coupling of asymmetric disk array-composites [1]; and (b) stiffness engineering via strategic geometrical cuts [2] [3].

The disk array resoswitch of Fig. 1(a) generates displacement gain by coupling an input disk array-composite to an output one (using a single disk in Fig. 1(a)) via a quarter-wavelength beam that effectively balances the energy on both sides. Since the stiffness of the 4-disk half-wavelength-coupled input array (n_{in} = 4) in Fig. 1(a) is four times larger than that of the single output disk (n_{out} = 1), the output disk must move more than the input ones to possess equal energy—specifically, $\sqrt{n_{in}/n_{out}}$ = 2× more—thereby providing displacement gain. So far, the only demonstrated such mechanical circuit of [1] utilized radial mode disk resonators, which constrained its Q to only 10,500. Based on [8], a wine-glass disk based version should do much better, but this has yet to be demonstrated.

On the other hand, the slotted-disk of Fig. 1(b) generates displacement gain by cutting slots along one axis (i.e., the output axis) of a wine glass disk thereby lowering the stiffness in that direction, hence raising its displacement relative to that along the orthogonal input axis. The result: displacement amplification in a single mechanical structure. Unfortunately, the slots induce higher energy losses at the slot-induced stressed corners, which degrade Q to ~10,000, which is many times smaller than commonly exhibited by non-slotted wine-glass disks.

The elliptic resoswitch of Fig. 1(c) basically engineers stiffness in a similar manner as the device of Fig. 1(b), except without the use of slots. Instead, it effects differences in orthogonal axial stiffness via geometric ratioing of the ellipse aspect ratio AR (a/b), where the smaller stiffness along its longer output axis yields a larger displacement than that along its shorter, hence stiffer, input axis. Unlike

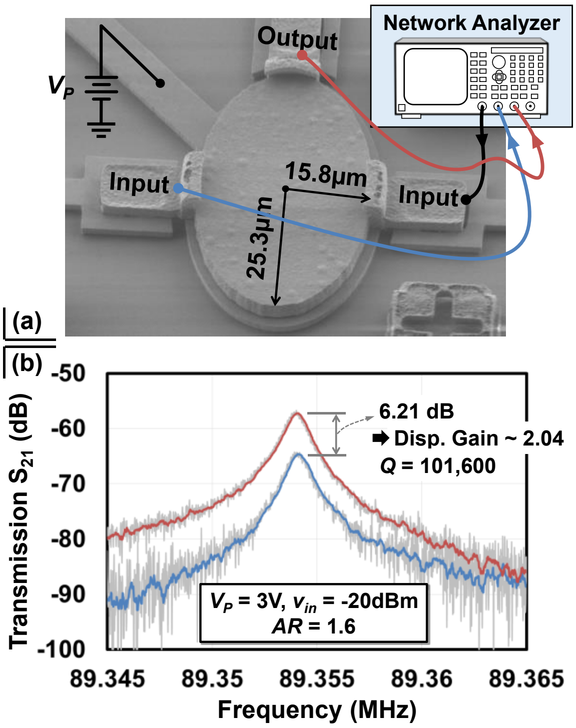

Fig. 4: (a) SEM of a fabricated polysilicon elliptic disk with an AR of 1.6. Measurement set-up for extracting displacement gain is indicated. (b) Measured transmissions obtained via the device and set-up in (a), exhibiting a displacement gain ~2.04 and a measured Q over 100,000.

the slotted disk, the elliptic disk avoids the energy-consuming stress corners of slots, allowing it to retain high Q. Fig. 3 compares the FEM-simulated mode shapes of the new design in (c) with those of (a) a conventional wine-glass disk and (b) the slotted disk, showing no displacement gain in (a), but (by red coloring) ample output displacement gain for both the slotted and the elliptic disks.

DISPLACEMENT GAIN MODELING

Unlike a slotted-disk, for which displacement gain depends on the size, location, as well as shape of its slots, making modeling very complex; the elliptic disk presents a much simpler structure, for which displacement gain depends only on its geometric aspect ratio AR and the Poisson ratio v of its structural material. A semi-empirical model based on FEA that predicts the displacement gain as a function of these two parameters takes the form

$$G_{disp} = AR^{-4.73v+2.626} \quad (1)$$

The basic form of (1) derives from knowledge that a purely circular disk (AR = 1) has an orthogonal axis displacement gain of one regardless of the value of Poisson ratio.

EXPERIMENTAL RESULTS

Elliptic displacement amplifiers were fabricated using a polysilicon surface micromachining process similar to that of [8]. Table 1 summarizes the designs, which span AR values from 1 to 2. Note that all elliptic disk designs have a fixed ellipse area of 400π μm^2 (i.e., πab) and their resultant resonance frequencies span from 96.5 MHz for AR = 1 to 82.4 MHz for AR = 2. Fig. 4(a) presents the SEM of one such fabricated elliptic device with AR = 1.6.

Table 1: Summary of Elliptic Disk Designs

a, b (μm^2)	ab = 400					
Thickness h (μm)	3					
Stem Radius (μm)	1					
Stem Height (μm)	0.7					
Aspect Ratio AR	1	1.2	1.4	1.6	1.8	2.0
Frequency (MHz)	96.49	95.36	92.68	89.31	85.79	82.40

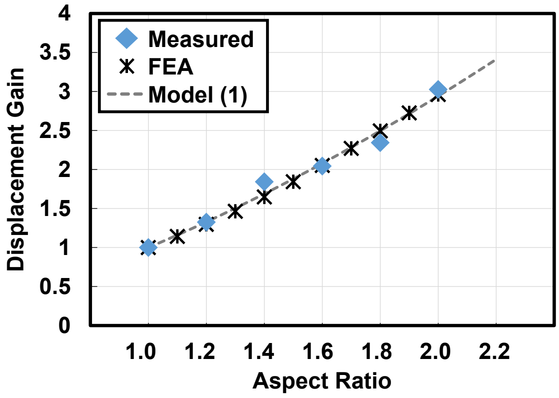

Fig. 5: Comparison of displacement gains as a function of aspect ratio obtained from measurement, FEA, and prediction using (1).

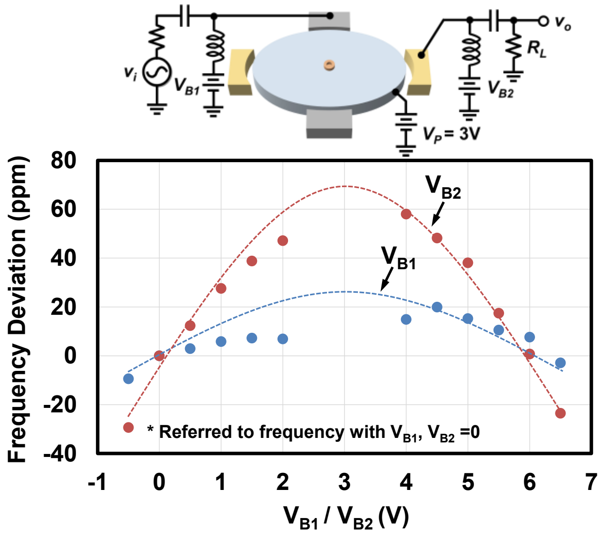

Fig. 6: Measured frequency shifts with tuning voltages applied on input (V_{B1}) versus on output (V_{B2}), where the lower mechanical stiffness along the output axis yields a larger tuning range.

Devices like this were measured under 10^{-5} Torr vacuum provided by a turbo pump using the indicated circuit, where one input electrode is connected to port 1, and the other input electrode and the output electrode are connected to port 2 and 3, respectively. Fig. 4(b) presents measured frequency transmissions between two input ports (S21) (blue) and between the input and output ports (S31) (red) of an elliptic disk with AR = 1.6, where the transmitted power difference between the two peaks indicates a displacement gain of ~2.04.

Fig. 5 plots measured displacement gain as a function of aspect ratio AR varying from 1 (a purely circular disk) to 2 alongside predictions by FEA and Eq. (1) (with ν = 0.226), showing good agreement. Here, a single elliptic disk with AR=2 achieves a displacement gain up to ~3.

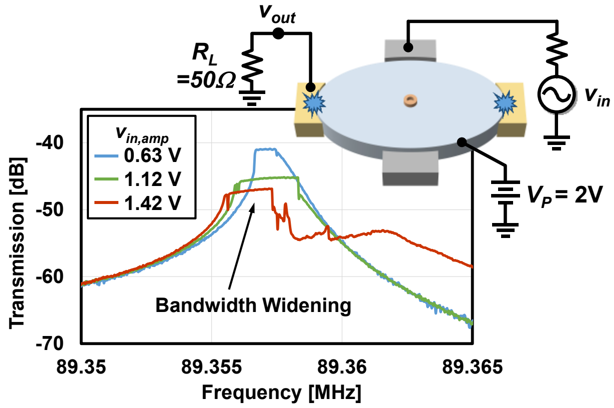

Fig. 7: Measured input to output frequency response spectra as a function of input drive voltage, showing flattening and bandwidth widening of the response at the onset of impacting.

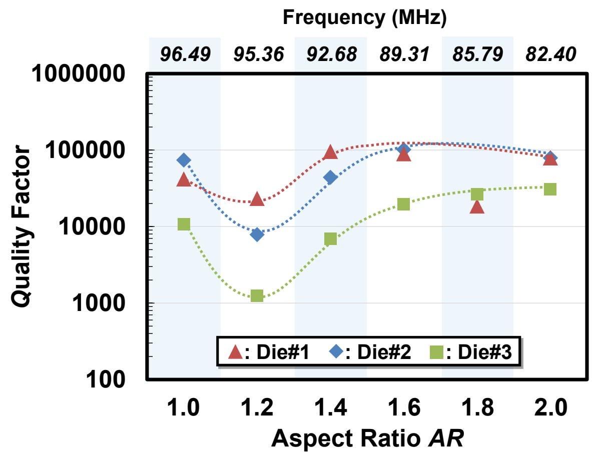

Fig. 8: Measured Q versus aspect ratio from three dies. Here, AR=1 corresponds to a circular disk, while higher AR's indicate ellipses. AR=1.2 presents the lowest Q while AR>1.6 seems to be able to recover Q back to that of a circular disk.

Fig. 6 plots the frequency shift versus electrical-stiffness tuning voltage applied at the input electrode (V_{B1}, blue curve) and the output electrode (V_{B2}, red curve), where the larger frequency shift of the latter confirms lower stiffness along the output axis. Fig. 7 presents measured frequency responses taken at the output electrode of an 89-MHz elliptic resoswitch as a function of increasing input voltage, showing the expected peak flattening as the elliptic disk impacts the output electrode.

ELLIPTIC DISK Q

Fig. 8 plots measured Q as a function of AR for several elliptic disks spanning 82.4-96.5 MHz on three different dies, indicating similar Q variations regardless of their Q magnitudes. Interestingly, when AR = 1.2 Q drops consistently from that of a conventional circular wine glass disk (AR = 1), but increases afterwards as the AR rises.

The measured Q of 100,000 for a 96-MHz AR=1 circular disk is short of the expected intrinsic Q limit, most likely due to a combination of anchor loss and phonon-phonon interaction loss [9] [10] [11]. Since phonon-phonon interaction energy loss is less influenced by geometry, the reduction in Q as AR changes from 1 to 1.2 likely results from anchor dissipation. In particular, the center stem dissipates

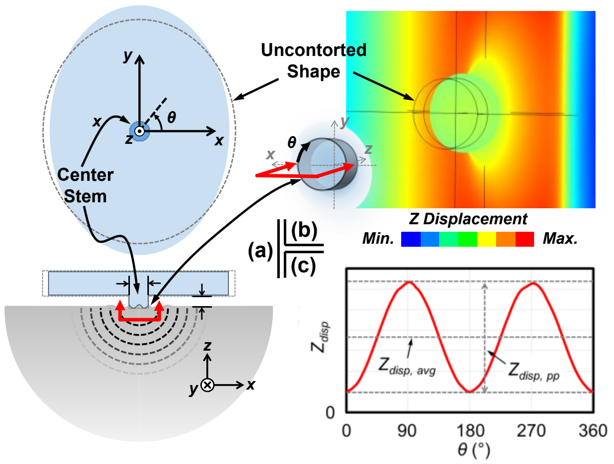

Fig. 9: (a) Schematic of an elliptic disk dissipating energy into the substrate while vibrating. (b) FEA-simulated deformation of the center stem bottom (substrate is not shown for clarity). (c) Illustration of z displacement components versus rotating angle along the circumference at the bottom of the center stem when the elliptic disk vibrates in the wine glass mode shape.

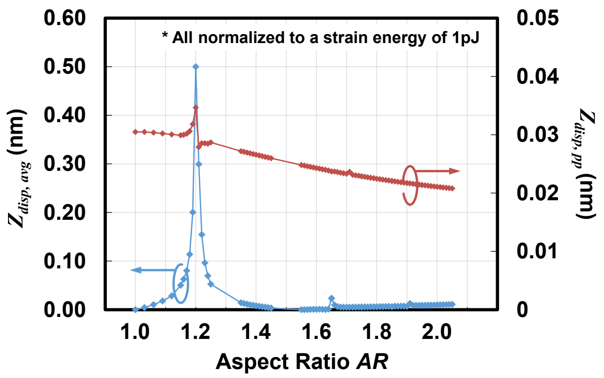

Fig. 10: FEA-simulated z-displacement components versus aspect ratio, indicating a large vibration magnitude along the z axis when AR = 1.2.

energy into the substrate via z-directed motion perpendicular to the substrate surface, as illustrated in Fig. 9(a).

Fig. 9(b) and (c) plot the FEA-simulated mode shape around the anchor area and the z displacement amplitude as a function of angle θ for a point along the circumference of the bottom of the center stem where it attaches to the substrate. Here, the z displacement comprises an average component $Z_{disp,\ avg}$ and a varying one with peak-to-peak magnitude $Z_{disp,\ pp}$. An increase in either component raises the amount of energy lost to the substrate, thereby lowering Q.

Fig. 10 plots the simulated z-displacement components, $Z_{disp,\ avg}$ and $Z_{disp,\ pp}$, as a function of θ for elliptic disks with varying AR values. Here, the simulated 1 μm-radius, 0.7 μm-tall center stem seems to best couple the vibrating energy of the 95-MHz elliptic disk when the $AR = 1.2$, which produces the largest $Z_{disp,\ avg}$, as shown in Fig. 10. This observation aligns well with the measurement results of Fig. 8 where the elliptic disks with an $AR = 1.2$ yield the lowest Q's.

In addition, aside from the circular disk case ($AR = 1$), $AR = 1.6$ yields the smallest $Z_{disp,\ avg}$, which might explain why this AR yields the highest measured Q's for two of the curves in Fig. 8. For $AR > 1.6$, on the other hand, although $Z_{disp,\ avg}$ magnitudes rise as AR increases, $Z_{disp,\ avg}$'s decrease, perhaps cancelling the former and allowing Q's on par with that of $AR = 1.6$, as shown in Fig. 8.

CONCLUSIONS

By engineering stiffnesses via dimensional ratioing rather than slots, the demonstrated elliptic disks provide an alternative method to achieve displacement amplifying resoswitches that retain high resonator Q's exceeding 100,000 that should improve the sensitivities of resoswitch-based zero-quiescent power radios at VHF. In fact, the almost 10× improvement in Q over previous disk array and slotted disk approaches should yield sensitivity reductions (i.e., improvements) on the order of 10dB. Of course, this work presented only polysilicon elliptic resoswitches with high contact resistances that preclude use in many desired applications. To be useful in an actual zero-quiescent power radio, next generation devices should employ metals or other more conductive materials at their contact interfaces. Methods for doing so without sacrificing Q are currently under study.

Acknowledgment: This work was funded by DARPA under the N-ZERO program.

REFERENCES

[1] Y. Lin, *et al.*, "Digitally-specified micromechanical ...," in *15th Int. Conf. on Solid-State Sens., Act., & Microsyst. (TRANSDUCERS'09)*, 2009 pp. 781-784.

[2] B. Kim, *et al.*, "μmechanical resonant displacement gain stages," in *22nd Int. IEEE MEMS Conf.*, 2009, pp.19-22.

[3] W.-C. Li, *et al.*, "Metal micromechanical filter-power amplifier utilizing a displacement-amplifying resonant switch," in *17th Int. Conf. on Solid-State Sensors, Actuators, & Microsystems (Transducers'13)*, 2013, pp. 1445-1448.

[4] R. Liu, *et al.*, "Zero quiescent power VLF mechanical communication …," in *18th Int. Conf. on Solid-State Sens., Act., & Microsyst. (Transducers'15)*, 2015, pp. 129-132.

[5] J. Johler, "Propagation of the Low-Frequency Radio Signal," *Proc. of the IRE,* vol. 50, no. 4, pp. 404-427, 1962.

[6] Y. Chen, *et al.*, "Ultra-low power time synchronization using passive radio receivers," in *10th Int. Conf. on Information Processing in Sensor Networks (IPSN)*, 2011.

[7] Y. Lin, *et al.*, "The micromechanical resonant switch ("resoswitch")," in *2008 Solid-State Sen., Act., & Microsyst. Workshop*, (Hilton Head'08), 2008, pp. 40-43.

[8] Y.-W. Lin, *et al.*, "Series-resonant VHF micromechanical resonator reference oscillators," *IEEE J. Solid-State Circuits,* vol. 39, no. 12, pp. 2477-2491, 2004.

[9] W.-C. Li, *et al.*, "Quality factor enhancement in micromechanical resonators at cryogenic temperatures," in *15th Int. Conf. on Solid-State Sensors, Actuators, & Microsystems (TRANSDUCERS'09)*, 2009, pp. 1445-1448.

[10] R. Tabrizian, *et al.*, "Effect of phonon interactions on limiting the f.Q product of micromechanical resonators," in *15th Int. Conf. on Solid-State Sensors, Actuators, & Microsystems (Transducers'09)*, 2009, pp. 2131-2134.

[11] J. E.-Y. Lee, *et al.*, "Study of lateral mode SOI-MEMS resonators for reduced anchor loss," *J. Micromech. Microeng.*, vol. 21, no. 4, p. 045010, 2011.

CONTACT

*Wei-Chang Li; wcli@eecs.berkeley.edu